Solid Earth Discuss., 6, 679–729, 2014
www.solid-earth-discuss.net/6/679/2014/
doi:10.5194/sed-6-679-2014

Solid Earth
Discussions
Open Access

Thermal characterization of the active layer at the Limnopolar Lake CALM-S site on Byers Peninsula (Livingston Island), Antarctica

M. A. de Pablo[1], **M. Ramos**[2], **and A. Molina**[1,3]

[1]Department of Geology, Geography and Environment, University of Alcalá Madrid, Spain
[2]Department of Physics and Mathematics, University of Alcalá Madrid, Spain
[3]Centro de Astrobiología, CSIC/INTA, Madrid, Spain

Received: 27 December 2013 – Accepted: 7 January 2014 – Published: 5 March 2014

Correspondence to: M. A. de Pablo (miguelangel.depablo@uah.es)

Published by Copernicus Publications on behalf of the European Geosciences Union.

Abstract

The Limnopolar Lake CALM-S site (A25) is the unique location on Byers peninsula where the active layer thickness is systematically monitorized (by mechanical probing during the thaw season and by temperature devices continuously since 2009). An air, surface, snow and ground temperature monitoring devices have been installed to monitor ground thermal behavior. We analyzed these data to present there the active layer thermal characterization. We use the air and ground mean daily temperature data to define the following parameters: maximum, minimum and mean temperatures at the air and at different depths, the zero annual thermal amplitude depths and position of the top of the permafrost table. The freezing and thawing seasons (defining their starting dates as well as their length), and the existence of zero curtain periods has been also established. We also derive apparent thermal diffusivity and plot thermograms to study the thermal behavior of the ground at different depths. After this complete thermal characterization of the active layer, we propose the potential existence of a permafrost table at about 130 cm in depth as well as the transitional zone above it, and discuss the role of water in connection with the thermal behavior of the ground during the study period.

1 Introduction

In Early February 2009, a new monitoring site following the protocols of the Circumpolar Active Layer Monitoring South (CALM-S) program (e.g., Brown et al., 2000; Matsuoka and Humlum, 2003; Nelson et al., 2004; Matsuoka, 2006) was established in the Limnopolar Lake basin (62°34′35″ S, 61°13′07″ W) (Fig. 1), in Byers Peninsula, Livingston Island (South Shetland Archipelago), Antarctica (de Pablo et al., 2010). This CALM site, named Limnopolar Lake, was officially added to the international CALM network in 2012 such as the A25 site in Antarctica (Appendix A). The scientific objective of this experience is to contribute to the international network to study the effect of global climate evolution about active layer thermal behavior similarly to the CALM

SED
6, 679–729, 2014

experiences located in Deception Island, at South Shetland Archipelago (Ramos et al., 2009a, b, 2014; Ramos and Vieira, 2009; Vieira et al., 2010). Similarities on surface grain-size distribution and texture, site elevation, local climate and site latitude, could allow us to determine the effect of both, the possible geothermal flux in Deception Island (an active volcano; e.g., Vila et al., 1992; Pallás et al., 2001) on the Active Layer Thickness (ALT), and the higher water content of the Limnopolar Lake CALM-S site. To complete the ALT monitoring in the Limnopolar Lake CALM-S site, we installed different instruments to monitor the ground thermal behavior on two shallow boreholes (85 and 135 cm depth) as well as the air temperature and snow coverage (de Pablo et al., 2010, 2013a; Table A1). The results of the first two years of ALT monitoring, in the Limnopolar Lake CALM-S site (de Pablo et al., 2013a), showed that the mechanical probing measurements correspond, not to ALT but to thawing depth (TD) because the bottom of the main borehole (130 cm depth) does not reach the depth of the top of the permafrost. This conclusion was based on the thermal data from the sensors installed in the boreholes, showing that if permafrost existed, it should be located deeper than 1.35 m, i.e., deeper than the total depth of our boreholes and the standard steel probe (100 cm) that we use to measure the ALT by mechanical probing.

Now, after five years of monitoring we have four complete years of air, surface, and ground temperature data (2009–2012). We use here some of those data (air and ground temperature from the deeper borehole) to conduct the first detailed analysis of the ground thermal behavior at this CALM site, extending and completing the preliminary results we obtained after the first two years of monitoring (de Pablo et al., 2013a). The objectives of this characterization are: (1) to establish the annual ALT, (2) to analyze the presence of permafrost below the active layer, or the deep it should be located in case of existence, (3) to determine the depth of zero annual thermal amplitude, the thermal and surface offsets, the apparent thermal diffusivity of the ground materials, the freezing and thawing indexes and the n-factor, as well as their evolution along the time for the study period; and (4) to analyze the ground thermogram for each year to locate possible depths with different thermal behaviors. This thermal characterization

SED
6, 679–729, 2014

is the base for future research works in this CALM-S site, as well as for the comparative analysis with the Crater Lake CALM-S site on Deception Island.

2 Study area, data and methods

2.1 Study area

The Limnopolar Lake CALM-S site is located in the smooth undulated plateau (about 105 m a.s.l) of Byers peninsula, Livingston Island, near the SW shore of the Limnopolar Lake (Fig. 1). This peninsula is the largest non-glaciated area in the South Shetland Archipelago, and it lies near the climatic boundary of permafrost (Bockheim, 2006; Vieira et al., 2010), i.e., an area where permafrost and active layers are strongly sensible to small temperatures changes. The climate in Byers peninsula is characterized by a mean annual air temperature of −2.8 °C (Bañon, 2001; Toro et al., 2007; Bañón et al., 2013), with extreme temperatures of −27.4 and 9.3 °C, but during the summer season, air temperature is 1 °C. Total annual precipitation is estimated to be 800 mm, and the snow covers the area for 7–8 months a year. Under that conditions, permafrost could exist, as well as an active layer whose existence is revealed by the presence of extensive periglacial landforms in the area (patterned grounds, stone circles, etc.), (López-Martínez et al., 1996; Serrano et al., 1996).

From the geological point of view, this region is characterized by Upper Jurassic–Lower Cretaceous volcanic, volcanoclastic and sedimentary materials and intrusive igneous bodies and Quaternary sediments (López-Martínez et al., 1996), latter affected by periglacial, glacial, fluvial, and weathering processes affected the bedrock after the deglaciation of the Peninsula over 5000 yr ago (Björck et al., 1996; Toro et al., 2013). The CALM site surrounding area is characterized by a mantle of gravels, sands, and debris, locally forming stone circles, polygonal terrains, patterned ground, and other periglacial landforms (López-Martínez et al., 1996, 2012; Otero et al., 2013). The CALM-S site (Fig. 2) is located on the unsorted sandy-gravel (locally forming pat-

SED
6, 679–729, 2014

terned grounds) east-facing flank of a small smooth ridge inside the Limnopolar Lake basin, about 2 % in slope, with a variable water table (locally as shallow as 5 cm at the lower part of the site), and without outcrops.

2.2 Data and methods

One of the main goal of the present study is based on the use of temperature data acquired by different sensors (air and ground) installed in early February 2009, and maintained yearly during the Spanish Antarctic campaigns. The Limnopolar Lake CALM-S site includes different instruments to measure air temperature, snow thickness (by air temperature at different heights in a thermal-snow-meter; de Pablo et al., 2010), surface soil temperature and ground temperature at different depths in two boreholes (Table 1). Additionally, we also have an automatic camera what takes one picture per day (at noon), to monitor the weather and snow cover evolution. We focus our attention on the ground thermal characterization for this reason we use air and ground temperatures acquired hourly; by a tinytag device (Gemini) for air temperature, and every three hours by DS1922L ibuttons devices (Maxim) for ground at different depths in the 135 cm depth borehole. All the characteristics of temperature devices are showed in Table 1 (and Table A1). Raw air and ground temperatures data (Fig. 3) were used to obtain mean daily values, and to calculate different thermal parameters as well as to produce plots to help us to understand the thermal behavior of the ground. Most of the calculations and plots here presented are based on the use of the preliminary version of CALM-DAT software (de Pablo et al., 2013b) and an Excel spreadsheet (by Microsoft).

We produced a thermal profile of the ground, what provides: (a) quick look of active layer existence and its depth, (b) permafrost existence, and depth of zero annual thermal amplitude. Annual maximum temperature values from the deeper sensors in the borehole (40, 70, 100 and 130 cm) were fitted to a linear curve in order to derive the depth of the active layer by extrapolation, and the depth of the top of the permafrost. Temperature amplitudes (during a selected period) were plotted vs. depth in order to

SED
6, 679–729, 2014

fit and exponential curve (Fig. 4) and to derive, the depth of the zero annual thermal amplitude by the use of the solution of the one-dimensional heat transfer problem with sinusoidal temporal evolution of the surface temperature in a homogeneous medium (e.g., Andersland and Ladanyi, 2003):

$$A(x) = A_0 \cdot e^{-\frac{x}{d}} \quad (1)$$

$$d = \sqrt{\frac{P \cdot \alpha}{\pi}} \quad (2)$$

where A is the thermal amplitude (in °C) and P the period (in s) at the surface temperature evolution, x is the position variable, depth (in m), and α the thermal diffusivity (in $m^2 s^{-1}$).

On the other hand, mean air and ground temperatures were used to calculate thermal and surface offsets (Fig. 5). Surface offset has been calculated in two different ways; first as the difference on the mean annual temperatures at the surface (2.5 cm depth) and the mean annual air temperature (160 cm height). However, the thermal offset, what is defined such as the difference between the mean annual temperature in the surface and the temperature at the top of the permafrost could not be directly calculated since our previous results point to we do not reach the top of the permafrost in the 130 cm depth borehole (de Pablo et al., 2013a). In spite of that, we approach the thermal offset by using in its calculation the mean annual temperature of the ground at the deeper point in our borehole (130 cm). The result should be considered such as an approach better than a real thermal offset.

Freezing and thawing periods were defined such as the date in which the mean daily temperatures remain below 0 °C or above it, respectively, ignoring short travels through this temperature inside each period. The length of each period is showed in days (Fig. 6). We did not considered the length of the 2009 thawing and 2012 freezing seasons due to the available data are incomplete for those periods because instruments were installed at the middle of the 2009 thawing season, and last data were recovered during the 2012 freezing season. Since the data does not represent the

SED
6, 679–729, 2014

complete season, we did not used them to calculate season length in days, but they were used to define the dates of the seasons limits, as well as the zero curtain periods.

Moreover the limit of the thermal seasons, we also defined the limits of the zero curtain periods which reflect the transitional period in which the energy exchange between soil and atmosphere is used to melt the ice existing in the ground (latent heat) better than increase the ground temperature (Fig. 7). This period is defined graphically such as the date in which the mean daily temperatures below 0 °C increase quickly to reach and remain at 0 °C for few days, the length in days of each one of those period at different depths were plotted to analyze their existence, behavior and evolution.

Mean daily temperatures of the air and the ground were also used to calculate and plot (Fig. 8) the freezing and thawing indexes (FDD and TDD, respectively), such as the summation of the negative (< 0 °C) (FDD) and positive (> 0 °C) (TDD) temperatures along the freezing and thawing seasons, respectively.

$$\mathrm{FDD} = \sum_{\text{Freezing}} (\overline{T} < 0\,^{\circ}\mathrm{C}) \tag{3}$$

$$\mathrm{TDD} = \sum_{\text{Thawing}} (\overline{T} > 0\,^{\circ}\mathrm{C}) \tag{4}$$

where T is the mean daily temperature (°C).

In order to compare with the previously described calculation for the depth of the top of the permafrost, thawing index were plotted vs. depth and fitted to calculate by extrapolation the depth in which the ground have not positive temperatures (Fig. 8). Freezing and thawing indexes of the surface (by the use of the temperature data at the shallower depth in the borehole: 2.5 cm depth) and the air (160 cm height) were used to calculate and plot (Fig. 9) the freezing and thawing n-factor (n_f and n_t, respectively)

SED
6, 679–729, 2014

such as the ratio between them (e.g., Andersland and Ladanyi, 2003).

$$n_f = \frac{\text{FDD surface}}{\text{FDD air}} \quad (5)$$

$$n_t = \frac{\text{TDD surface}}{\text{TDD air}} \quad (6)$$

Plots of cumulative daily *n*-factors have been developed to characterize and compare the evolution of the freezing and thawing periods in the study area, as well as to define the mean value what characterize the thermal behavior of the soil surface in the area.

Apparent thermal diffusivity for the freezing and thawing seasons were also calculated. We used the temperature of the ground at different depths, we selected few-days long periods for each season in which the temperature evolution showed a well defined sinusoidal wave to calculate the soils apparent thermal diffusivity. Then, we used the available data in this period to derive, applying the Eqs. (1) and (2) in two different depths (X), the thermal diffusivity (α) by means of the amplitude method summarized in the next equation (e.g., Andersland and Ladanyi, 2003):

$$\alpha = \frac{\pi}{P} \cdot \left[\frac{X_2 - X_1}{\ln\left(\frac{A_{X_1}}{A_{X_2}}\right)} \right]^2 \quad (7)$$

where P is the considered period (s), X is the space variable, depths (m), and A the thermal amplitude (°C). Finally, raw ground temperature data were plotted in a thermogram (temperature at depth vs. time), as well as the 0 °C isotherm in order to study the ground thermal behavior and its evolution (Fig. 3).

SED
6, 679–729, 2014

3 Results

3.1 Thermal profiles

Thermal profiles show a v-shape design due to a decreasing temperature range between maximum and minimum temperatures with the depth (Fig. 4). However, maximum and minimum temperature curves are asymmetrical respect the mean temperatures and also respect 0 °C isotherm, what remain approximately constant along the depth of the borehole (Table 2). This mean temperature is lower than 0 °C (about −1 °C) in 2009 and 2011, but slightly lower than 0 °C in 2010 and 2012.

Overlapped to this asymmetry, a change along the time of the thermal amplitude for each depth could be also observed. Near the surface, the thermal amplitude increase in 2009–2012 period from 17 °C to 26 °C. However, clear change trends are not observed in deep, and increasing and decreasing amplitudes could be observed. Smaller thermal amplitudes occur in 2010 and 2012, were it is as low as 10 °C, for all the depths, although especially at deeper sectors.

In detail, the shape of the curves of the maximum and minimum daily temperatures along each year is also asymmetrical. On the first hand, both have different pattern for the first 40 cm with a non-linear curve, and for the 70–130 cm depths, with a linear curve. That asymmetry is recognizable in 2010 and 2011. In 2012, there are not data for 40 cm depth sensor, what explain the gap in the curves at that depth. The slope (thermal gradient) of the deeper sectors (70–130 cm) of the curves is lower in 2010 and 2012 due to the approximately constant minimum temperature in deep, especially in 2010. On the second hand, the curves of maximum and minimum temperatures are also different with a more pronounced curvature in the case of the positive temperatures, marking the higher thermal amplitude of positive temperatures.

In any case, the thermal profiles show that, for any year of the study period, the maximum temperature curves do not reach the 0 °C isotherm in the first 130 cm depth. However, in 2010 and 2012, the maximum temperature is near that isotherm, especially considering the ±0.5 °C of the sensors accuracy.

SED
6, 679–729, 2014

Finally, maximum and minimum temperatures neither converge what means that the zero annual thermal amplitude depth was not reached by the 130 cm deep borehole, and its calculation is required, such as we show below. In spite of that, this characteristic depth should be shallower in 2010 and 2012, when the thermal amplitude at 130 cm depth is as small as 1 °C.

3.2 Top of permafrost depth

Maximum of the mean daily temperatures registered by the deeper sensors installed in the borehole (i.e., 40, 70, 100 and 130 cm) could be used to deduce by linear extrapolation the depth in which the permafrost, if it exist, should be located. We fitted those values to a linear curve in a temperature vs. depth plot, in order to calculate the intersection with 0 °C isotherm (Fig. 4). The results are that the maximum temperatures should reach 0 °C, at 145, 124, 130 and 135 cm depth, from what we deduce that the depth of the top of the permafrost could be located at a mean depth of 134 ± 22 cm at the study site during the 2009–2013 study periods.

3.3 Zero annual thermal amplitude depth

Based on the temperature amplitude at different depths for each year (Table 2), we fitted an exponential curve following the Eq. (1) (Fig. 4) in order to derive the depth of zero annual thermal amplitude, i.e., the depth at which any climatic variation with periods smaller than one year is completely attenuated (at the range of the inverse of e). We obtained values of d for 2009 to 2012 yr, and assuming that the depth of zero annual thermal amplitude is about $3 \cdot d$, derived zero annual thermal amplitude depth is about 2.2 ± 0.2 m, 1.4 ± 0.1 m, 2.0 ± 0.2 m and 1.3 ± 0.1 m, respectively for the 2009 to 2012 yr. Those results agree with what is showed in the thermal profiles, with higher thermal amplitudes at 130 cm deep in 2009 and 2011, than in 2010 and 2012 (Fig. 4).

SED
6, 679–729, 2014

3.4 Thermal and surface offsets

The mean annual temperatures at different depths in the ground, as well as the mean annual temperature of the air at 1.6 m in height, (Table 2) were used to derive both the thermal offset (surface–top of the permafrost), and surface offset (air–surface) (Table 3; Fig. 5). We obtained absolute values of 0.4 °C, 0.0 °C, 0.3 °C and 0.2 °C for the thermal offset in 2009 to 2012, respectively, with a mean value of 0.2 ± 1 °C. On the other hand, we also obtained (in absolute values) 1.8 °C, 1.5 °C, 1.7 °C, and 1.8 °C for the surface offset in the same years, respectively, (Fig. 5) with a mean value of 1.6 °C ±1 °C. Both offsets show a similar pattern with lower absolute values in 2010, and a difference between them of about 1.7 °C. The mean absolute value of the thermal offset is 0.2 °C meanwhile the mean surface offset is 1.7 °C.

3.5 Freezing and thawing seasons

Plots of air and ground temperatures (Fig. 3) made possible to define the limits of the main thermal seasons what characterize this polar region: freezing and thawing. The limits dates of those seasons are defined by the change of the temperature from positive to negative (start of the freezing period), or from negative to positive (start of the thawing period).

The starting dates of each period (Table 4) are approximately similar for the upper depths, but something different in the lower ones, following the slopes previously calculated of 50 and 40 days m^{-1} in difference. In general, freezing season starts between 13 March and 22 March at the surface, and between 10 June and 15 July at 130 cm deep. Thawing season starts between 13 December and 31 December at the surface, and between 2 January and 6 February at 130 cm deep. The longer freezing season occurred in 2010, meanwhile the longer thawing season was registered in 2012.

The ground at different depths shows thawing and freezing periods with well defined lengths, of about 73±2 days of thawing season and 292±2 days for the freezing season (Table 5). Those values change with depth in the borehole, from the surface to 130 cm

SED
6, 679–729, 2014

in depth, ranging from 43 ± 2 to 93 ± 2 days in the case of the thawing season, and from 278 ± 2 to 314 ± 2 days in the case of the freezing season. In general, the shorter freezing period and the longer thawing period occurs in the surface, trending to invert with depth. The different behavior is observed at 130 cm depth, with similar lengths of the freezing and thawing period than in the surface (Fig. 6). In general thawing season shows more variable lengths than freezing season. The fitted linear curve to the mean season length values return a slope of about 50 days m^{-1} and 40 days m^{-1} in the variation of the thawing and freezing seasons lengths, respectively. We also used the lineal fitting curve of thawing period to deduce the depth at which the thawing period is 0 days in length, or, what is the same, the depth of the top of the permafrost. The result is about 180 cm depth. However, this approach does not consider the data of the deeper sensor (130 cm), what have a higher length of the thawing season and a shorter one of the freezing period than expected, i.e. they do not fit the trend of the depths above it. By the use of the fitting curve of the freezing length, we obtain a depth of 215 cm for the deep in which the length of the freezing season is 365 days.

3.6 Zero curtain periods

In all years, at the end of the freezing period, we observed on the mean daily temperatures the existence of zero curtain periods (Fig. 3). They tend to start at the same day in all depths, between 7 October and 19 November, or with a different, in general, smaller than 10 days (Table 6). Only the deeper sectors, at selected years, show a delay, starting the zero curtain periods in early December. The zero curtain period start with an increase of the temperatures at all depths at the same time, to reach 0 °C remaining at that temperature for period of about 76 ± 2 days (Fig. 7). However, there is a wide variability between the different depths, and for the different years, ranging between 35 ± 2 to 135 ± 2 days in length. The zero curtain periods are longer in deep (70 to 100 cm), except for the deeper ground in the borehole shows lengths similar, or even smaller, to the zero curtain period lengths in the shallower ground.

SED
6, 679–729, 2014

Moreover of the zero curtain period at the end of the freezing period (spring season), we observed that, except at shallower depths, the ground shows similar zero curtain periods during the fall season, in early freezing season. They are typically shorter of about 32 ± 2 days in length, but ranging between 25 ± 2 and 115 ± 2 days (Fig. 7). In difference with the zero curtain periods during the fall, their length increase with depth and they are not recognizable at the shallower depths. Moreover of this pattern, we observe abrupt differences the period length at 20 and 70 cm in depth, except in 2012. These zero curtain periods were longer in 2010 and 2012 (Table 6).

A peculiar event has been observed in 2012 when data reflect two zero curtain periods, in 19 August, and in 12 November 2012. The first event was about one month long, finishing in 8 September due to a new freezing process. Only the second one was long enough to possible conduct to the complete thaw of the ground. However, this process was not completed at the date in which the data sensors were recovered in 22 January 2013, clearly later than the end of the freezing season in the previous years (Table 6).

3.7 Freezing and thawing indexes

Freezing and thawing indexes (FDD and TDD, respectively) were calculated by the use of Eqs. (3) and (4) and summarized in Table 7. Resulting FDD values for the air ranges between -730 ± 73 and -1170 ± 117 °C day, meanwhile TDD values ranges between 72 ± 7 and 142 ± 14 °C day. On the other hand, FDD for the ground ranges from -664 ± 30 to -105 ± 50 °C day and the TDD ranges from 21 to 290 °C day. In general, higher values are reached at the surface, decreasing in depth (Fig. 8), and the air has higher (absolute) values of FDD but lower of TDD. In the first case, about the double than the higher FDD of the ground (at the surface), meanwhile the TDD is similar to those reached between 20 and 70 cm depth.

The evolution of those indexes along the study period shows an abrupt decrease on FDD and TDD values in 2010, and a slight decrease in 2012 (Fig. 8). Linear fitting reveals mean slopes of 21.3 ± 2 and 23.7 ± 14 °C day yr^{-1} for the TDD in the air and in

SED
6, 679–729, 2014

the ground, respectively, and mean slopes of 15.7 ± 2 and $32.2 \pm 16\,^{\circ}\mathrm{C\,day\,yr^{-1}}$ for the FDD in the air and the ground, respectively (Table 8). In the case of the TDD, a narrow change can be observed at 40 cm depth, meanwhile, in the case of FDD the values are approximately similar for all depths. The unique exception occurs at 70 cm depth, in which the FDD and TDD slope for the study period is indisputable higher than for the nearest depths, especially for the FDD (Table 8).

The higher values of TDD and FDD in the ground in 2010 and 2011 occur at all depths (Fig. 8), showing differentiated values patterns respect 2010 and 2012. Those differences are smaller for the TDD. The evolution of TDD and FDD with depth shows similar pattern than the thermal profiles (Fig. 4), although differences with depth are clearer for the FDD in 2009, where values shows a different pattern in depth than in the following years (Fig. 8). In the case of TDD linear fitting of the curves rises near the 0 °C day value at around 105 and 158 cm in depth (Fig. 8).

On the other hand, the difference between FDD and TDD provides a negative balance for all depths and years (Fig. 8). In general this balance shows the higher absolute values at shallow depths decreasing quickly to reach an about constant value, what is different for each year.

Described differences between 2009 and 2011 respect 2010 and 2012 are also evident at the daily cumulative plot (Fig. 8) with higher values in 2009 and 2011 and lower in 2012 for the FDD, meanwhile the TDD increase between 2010 and 2012 but with high values also in 2009. In detail, the FDD shows behavior common for all years, with a slight increasing (in absolute value) from late February to early March. Later values increase quickly until middle May, remaining about constant or slightly increasing until early June. From this date, the values increase quickly again until middle August where a new change on the increase velocity is marked in the curves. In some cases, at this date, a stop on the increasing is evident until to start a new increase on the values until the late freezing season. Finally, values increase slowly between October and November, and from here the daily cumulative values remain constant due to the end of the freezing season.

SED
6, 679–729, 2014

Daily cumulative TDD values show its own behavior with similar steps in the plot meanwhile increasing along the thaw seasons. In general, values start to increase at different dates, from late November to late December. Values increase about constantly until late February or early March, where the increase velocity decrease or is practically cero. Finally, in late March the daily cumulative TDD stop to increase, marking the end of the thaw season, and remaining constant during the immediately next freezing season.

3.8 *n*-factors

Calculated freezing and thawing *n*-factors (n_f and n_t, respectively) such as showed in Eqs. (5) and (6) for the freezing and thawing indexes (Table 7), show closed values for the different years of the study period. The n_f values are 0.54 ± 0.3, 0.4 ± 0.25, 0.57 ± 0.3 and 0.39 ± 0.2 for 2009 to 2012, respectively. On the other hand n_t values are 1.97 ± 1.2, 1.20 ± 0.7, 2.05 ± 1.2 and 2.06 ± 1.2, respectively for the same years (Table 9).

Daily cumulative *n*-factors for each year (Fig. 9) changes quickly at the beginning of the freezing or thawing seasons (freezing and thawing indexes are low and therefore more sensitive to added values; Karunaratner and Burn, 2003, 2004). Latter in the season, they oscillate between more constricted values. And finally trend to stabilize at the end of the season. Calculated n_f and n_t correspond to the value raised by them during the final stable period, meanwhile the mean n_f and n_t we also calculated provide higher values what depends of the amplitude of the oscillations showed along the respective season.

Evolution of n_f along the study period, shows similar patterns but differences are evident for each year. In 2009 and 2011, the n_f quickly increases from late march to reach an slightly lower value than what it will reach at the end of the season (final n_f) in few days. Later, the values start a new increase but less drastic what take about one month until early to middle April. After that, the values reduce in a variable ratio for about one or two weeks to slowly increase during about one month and a half to reach other maximum at about middle July. From this date, the values could rise a little

SED
6, 679–729, 2014

bit more until early September to October from when values slightly decrease trending toward a value what completely stabilize from middle November to early December. Final reached values correspond to the calculated n_f (Table 9). In case of 2010 and 2012, this behavior of the n_f is similar but at different dates and specific evolutions in early freezing season. The n_f values start to increase early, in middle February. However, in 2010, the increase of the values is not as quick as in 2009 and 2010, meanwhile in 2012, the increase is more drastic with a peak at late February, and then reducing again until late March. The main peak value is reached in 2010 in early May, meanwhile in 2012 is reached in late April. From that dates, the values reduce until early-middle June and from here they follow the same trend than in the previous years. The difference is the final value reached at the end of the stable phase, what is lower in 2010 and 2012 than in 2009 and 2011.

On the other hand, the evolution of the n_t values show two differentiated phases. The first one, corresponding to the thawing season in which the values decrease starting from early November to early December to increase again dramatically in a couple of weeks in early January followed by a similarly dramatic decrease in late January. From here, values increase or decrease (depending of the year) until the end of the thawing season in late February to late April From this date, the values remain completely stable for all the freezing season. The values of this stable phase correspond to the calculated values by the use of the freezing and thawing indexes better than the global values (Table 9).

3.9 Thermogram

Thermograms provide a visual approach to the thermal evolution of the ground at different depths (Fig. 3). The thermograms of the study are for the 2009–2012 period show how the freezing reach the bottom of the borehole, and how the thawing affect also affect to all the monitored depths. 0 °C isotherm reveals when and how the freezing and thawing events occur at different depths. Moreover, this type of plot also provides

SED
6, 679–729, 2014

an idea of the temperatures ranges reached by the ground in each moment and its evolution.

The thermograms shows how the ground reach lower temperatures in 2009 and 2011, reached −6.4 °C in the surface, and −2.7 °C at 130 cm depth, what made 2011 the cooler year of those registered in the data. On the other hand, 2010 and 2012 are the warmer years respect the ground, since the temperature it reaches is about −5.4 °C in the surface, and lower than −1.1 °C at 130 °C depth, what made 2010 the warmer year of the studied period.

These plots provide a visual confirmation of the previously described freezing-thawing seasons. The freezing season starts at the surface at around late March or early April, and finish at about late November or early December. In general, freezing occurs at different depths gradually taking about 2 months to reach the maximum registered depth (130 cm). In early freezing season, the low temperatures reach about 70 cm in few weeks, but higher temperatures warm the ground again, before the definitive and full ground freezing. This behavior is common in all the monitored years. A common characteristic of the freezing process is that it ever starts from the surface and evolve toward the deep.

On the other hand, thawing process follow a different behavior. Although the complete thawing of the ground occurs in about one month, it does not occur in a gradual process, but in a very quick events affecting only to a range of depths. Thermograms show the first few tens of centimeters (no more than 30 cm) are the first on increase their temperature above 0 °C meanwhile the rest of the ground remains freeze. This initial event occurs in 1–2 days. Only few weeks later, other sector of the ground thaw. Although thermograms are affected by the lag of data between 70 and 100 m in depth, we could observe how this second thawing event affects to the ground between 30 and 100 cm. In a similar way than the shallower ground, this event occurs in 1–2 days, meanwhile the lower ground still remain freeze. Finally, few weeks later, we have the complete thaw of the 130 cm of the studied ground. This pattern in the thawing evolution is evident in 2010 and 2011. In 2012 the freezing season was still not finish at the

SED
6, 679–729, 2014

moment of to recover the data from the loggers, and for that reason the thermograms only shows the thawing of the shallowest ground. On the other hand, in 2009, we observe how the process is similar, except by the thawing of the bottom depths few days earlier than the 30–70 cm sector.

In detail, the thawing of the shallowest ground does not start at the surface, but few centimeters below is, such as is visible in the thermograms, for example in early December 2009, middle November 2010, late November 2011, or middle December 2012. The thickness of these layer what thaw earlier than the surface, as well as its depth, is variable from one year to the other. But this process also occurs during the thawing events during the early freezing season, such as in early April 2009, middle March 2010, or even in late April and middle March 2012. In these events, the ground initially freeze during the early freezing season is thawed immediately below the surface, meanwhile the surface and deeper ground remains freeze.

3.10 Apparent thermal diffusivity

The main parameter describing the thermal properties of the materials of the ground is the thermal diffusivity. We calculated the apparent thermal diffusivity for the thawing season each year by the use of data from the sensor until 20 cm in depth. The resulting values (Table 10) range between $3.3 \times 10^{-7} \pm 0.2 \times 10^{-7}\,m^2\,s^{-1}$ in 2009 and to $5.6 \times 10^{-7} \pm 0.1 \times 10^{-7}\,m^2\,s^{-1}$ in 2012. During the freezing season, due to the absence of well-defined sinusoidal temperature signals in the data series (Fig. 13), it was only calculated in the 2010 freezing season obtaining a lower value of $1.86 \times 10^{-7} \pm 0.7 \times 10^{-7}\,m^2\,s^{-1}$.

4 Discussion

The here presented detailed results thermally characterize the ground of the active layer of the Limnopolar Lake CALM site, monitored between early 2009 and early 2013.

SED
6, 679–729, 2014

Those data could be used now to compare to other CALM sites in the region, such as this one located in Deception island, (e.g., Ramos et al., 2009a, b; 2014; Ramos and Vieira, 2009; Vieira et al., 2010; Ramos et al., 2014) to establish analogies and differences what could help to define the active layer characteristics (and permafrost depth) in the edge of the Antarctic continent, but also to contrast them with the regional weather and climate evolution in the South Shetland Archipelago area. However, those results are also necessary to allow comparative analyses with other CALM sites all around the world with similar thermal properties and environmental conditions (climate, geology, topography, vegetation), as well as the base for future frozen ground trend analyses taking into account the global warming scenarios.

Moreover this characterization, the detailed analyses of some of those results could help us to better understand the properties of the ground at this CALM site, fundamental for the correct interpretation of the results from the past and future active layer thickness monitoring in this CALM site (e.g., de Pablo et al., 2013a). For that reason, here we study in deep some of the results showed above.

Apparent thermal diffusivities of the materials in the Limnopolar Lake CALM site we calculated for the thaw season, 3.3 to 5.6×10^{-7} $m^2 s^{-1}$ (Table 10) are similar to the values obtained in previous calculations (de Pablo et al., 2013a), and are consistent with sedimentary materials and soils with significant water content (e.g., Campbell and Norman, 2000). Those values point in the same direction than the values we obtained for the thawing *n*-factor of about 2, what is the usual value for sand and gravels (see Andersland and Ladanyi, 2003 and references therein). However, both apparent thermal diffusivity on freezing season and freezing *n*-factors are lower than expected for the same materials. This reduction on the values could be related to high water content (ice) during the freezing season, because freezing *n*-factor for sand and gravel should be around 0.9, but we obtained values of about 0.45, what are approximately the value of sediments and soils under snow (see Andersland and Ladanyi, 2003 and references therein). The soils of the area in which the CALM site is located have been classified such as sandy loam (Otero et al., 2013) with sand contents of about 46 to 80 %, and

SED
6, 679–729, 2014

such as coarse sands well selected – SW at the Unified Soils Classification System – (Molina et al., 2013), what agree with our results and support our interpretations about the nature of the materials, and the description of surface materials (de Pablo et al., 2013a; Otero et al., 2013).

The high water content of the soils was evident during the fieldworks since ponds were visible at located sites of the Limnopolar Lake CALM site (those located at lower elevation), and the water table level during the thaw season could be as high as few centimetres (Fig. 2). Fieldworks at the end of the freezing season also revealed that the ground remain frozen and cemented by ice until the surface below the snow and ice layer covering the study area. Although we did not studied here the snow thickness evolution, previous works on this area revealed that the snow cover thickness could reach more than 80 cm (de Pablo et al., 2013a), what provides, during the thaw season, a significant volume of water what could explain the enrichment on water of the materials forming the ground.

Presence of water in the ground is also revealed by the long zero curtain periods we were able to define in the temperature data of the borehole (Fig. 7; Table 6). Zero curtain periods are usually related to ice melting because the received heat (from the sun and the atmosphere) is consumed on the phase change process of the water better than to increase the temperature of the materials of the ground (e.g., Andersland and Ladanyi, 2003). Then, the long zero curtain periods we observed at the end of the freezing season, as long as 90 days in the surface, imply high water content in the materials. Moreover, variable lengths of those zero curtain periods could be related to both differences in received heat, but also to different water content each year, probably due to differences on snow cover. However, zero curtain periods not only occur in the surface but at all depths in the ground (for the 130 cm we are able to monitor), with slight increasing lengths with depth (Fig. 7), what could be related to the delay on the thermal wave penetration, but, in any case, due to water content in the materials. A difference in this behavior could be observed at 130 cm depth, in which the length of the zero curtain periods at the end of the freezing period is about one third to a half

SED
6, 679–729, 2014

of the length of the same period at 100 cm depth. This behavior does not occur during the zero curtain periods at the early freezing season, where the shallower ground does not show this thermal behavior (Table 6).

Absence of zero curtain periods at shallower ground during early freezing period could be explained by the absence of water (at the borehole site). The complete melt of the snow cover in early thawing season, the subsurface water flow and the evaporation could dry the first 15 cm of the ground, meanwhile the rest of the terrain remains wet, what result on increasing zero curtain period at early freezing season (Table 6). This level is coincident with the level at which the 0 °C isotherm showed in thermograms (Fig. 3) firstly freeze during the early freezing period, and the first on thaw during the late freezing season. In fact, this level could be related to subsurface water flow during the early snow cover melting at the borehole location, since the date of this shallow level thaw is coincident with the date of the snow cover melting (such as seen on de Pablo et al., 2013a).

On the other hand, the lengths of zero curtain periods at the end of the freezing season are about similar for all depth (although slightly increasing with depth), except for the deeper ground (130 cm in depth), where the length is clearly lower such as we described above. We here propose that the existence of liquid water at this level in the ground could explain this behavior. The water coming from snow cover melt, could percolate in the ground until reach this depth melting quickly the ice before the thermal wave from the surface reach that depth. Thermograms (Fig. 3) show that, in general, the ground thaw from the surface to the deep at the borehole location. Then, the water could not come from the surface directly on top of the borehole, but from the surrounding area.

Pictures of the basin shows that the higher elevations of the ridge in which the CALM site is located are the first on lost the snow cover. The resulting melt water could percolate producing a subsurface flow due to the 2 % in slope of the area. Moreover, taking into account that the Limnopolar Lake CALM site is located at the top and a flank of a low ridge in the middle of a basin (Otero et al., 2013; de Pablo et al., 2013a), we

SED
6, 679–729, 2014

speculate that there is not a regional subsurface source of the water, and all the water what could contain the materials in the ground should remain there from one year to the other, or infiltrate from the surface due melt of the snow cover.

The reason this possible water flow occurs at that depth could be related, from our point of view, to the existence of permafrost (as an impermeable layer) below the active layer. We based this proposal on (1) the calculated depth of the top of the permafrost at about 134 cm depth, what agree with (2) the general reducing thawing period and indexes, and increasing freezing period and indexes with depth; (3) the ranges of depths at which the thawing season should be zero (if the ground remains constantly frozen), of about 180 cm; (4) the range of depths in which the TDD should be cero, of about 105 to 168 cm; (5) the null slope of the TDD along the studied period and the negative slope of FDD (increasing values trend); (6) the negative balance between TDD and FDD; (7) the stable negative mean temperature of the ground and (8) the temperatures near 0 °C at 130 cm depth as seen in the thermal profiles.

Although we could not confirm with our thermal data from the 130 cm depth borehole that there is a permafrost table below the active layer, we found its presence more reasonable than what we expected (de Pablo et al., 2013a), although a deeper borehole should be necessary to confirm and to monitor it. However, other regional studies confirm the presence of permafrost in Byers Peninsula (e.g., López-Martínez et al., 1996; Serrano et al., 1996) and, for that reason, the here proposed permafrost existence agrees with the regional context. We also had the direct evidence of a frozen table presence below the surface during the borehole drilling in February 2009. The drilling engine we used (STIHL BT 121) allows drill more than 2 m in sedimentary materials such as those forming the surface of both the Limnopolar Lake CALM site. However, it was really complex to drill from 110 to 138 cm, what it was the real maximum depth we reached at the borehole, due to the extremely hardness of the ice-cemented sediments. We directly observed that the bottom of the borehole was not rocks but frozen ground such as seen in the detritus from the drilling operations. However, at that mo-

SED
6, 679–729, 2014

ment, we were not able to establish if it was the top of the permafrost table or a still frozen sector of the active layer during the thawing season.

The increasing drilling complexity from 110 cm depth and the thermal behavior observed on the thermograms (Fig. 3), could, may be, point toward the presence of a transitional zone-like in the ground (e.g., Bockheim and Hinkel, 2005). Except near ponds in the CALM site, we never obtained deeper thawing depths of 100 cm when measuring the active layer thickness by mechanical probing (de Pablo et al., 2013a), and agrees with variable depths of the top of the permafrost we obtained for 124 to 145 cm, and the variable depth of the zero annual thermal amplitude depth, between 130 and 200 cm we calculated above. Thermographs also show how the ground below 100 cm in depth remain freeze for longer during the thaw season, although it finally melts in early February (except in 2013, when still remained freeze at that date).

In any case this possible permafrost table should be considered instable due to the mean temperatures of the ground: slightly lower than 0 °C at the first 130 cm of the ground (Fig. 4). Then, it is sensible to any change on the environmental conditions, especially air temperature and snow cover, what could produce a different thermal behavior in the ground, such as revealed by the thermograms (Fig. 3).

Finally, four years of data are not enough to analyze thermal trend of the ground, what, from different points of view, does not show a clear behavior in the study period. In fact, all the values and plots here described and discussed seems not to reflect a clear trend, but a peculiar behavior in which data from 2009 and 2011 shows about similar values, but different than those obtained by data from 2010 and 2012, such as seen on thermal profiles (Fig. 4), thermal amplitude (Fig. 4), the zero annual thermal amplitude depth, surface and thermal offsets (Fig. 5), FDD and TDD indexes (Fig. 8), or thermograms (Fig. 3) plots. However, the mean air temperature has been slightly increasing in the study period, as well as the TDD indexes and the thawing *n*-factor. Although we could not conclude it by the available data, the ground seems to increase its temperature. To extend the time series data and to drill a deeper borehole in the area is fundamental to study the thermal trend and to monitor the active layer and the

SED
6, 679–729, 2014

possible unstable permafrost layer and a possible transitional zone we propose to exist below it.

In any case, the different behavior we observed on the data during the study period points toward the important role than water play in the thermal evolution of the ground in this CALM site, probably due to the water infiltration from the surface due to snow cover melt. To analyze in detail this role should be necessary to confirm the differences observed each year, and to allow understand the future behaviors, we could observed on the further data analysis on future years.

5 Conclusions

The analyses of thermal data from air and ground at different depths allowed us to reach the objective of the present research: to characterize the thermal behavior of the terrain at the Limnopolar Lake CALM site.

We characterize this ground for the study period by the next parameters:

- The mean ground temperature ranges between about −1.2 °C and −0.2 °C, with thermal amplitudes of about 14 °C at the surface and 0.7 °C at 130 cm depth.
- The freezing season starts between middle March and early April, and have a length of about 290 days.
- The thawing season starts between late December to late February (depending of the depth), and have a length of 75 days.
- The TDD index of the ground ranges between 16 and 290 °C day meanwhile FDD index ranges between −105 and −664 °C day, gradually decreasing (in absolute value) with depth.
- Resulting freezing and thawing *n*-factors reveal values ranging between 0.39 to 0.54 and 1.2 to 2.06, respectively.

SED
6, 679–729, 2014

- The mean thermal offset is 1.6 °C meanwhile the mean surface offset is 0.2 °C.
- The apparent thermal diffusivity during the thaw season ranged between 3.3×10^{-7} and 5.56×10^{-7} $m^2 s^{-1}$, values what agree with sedimentary materials with significant water content.
- Zero curtain periods exist during on both early and late freezing seasons, marking the presence high water content in the ground.
- Length of zero curtain periods increase with depth until 135 days, except at 130 cm deep, showing similar values than in the surface during the late freezing season.
- Zero curtain periods at the end of the freezing season should start from early October to middle November.
- Depth of the top of the permafrost should be located at about 135 cm, and the Zero annual thermal amplitude between 140 and 220 cm in depth.
- Thermograms shows specific behaviors of the ground at different depths, especially the shallower 20 cm, the first on thaw at the end of the freezing season, and the ground below 100 cm in depth, which remains frozen for longer during the thaw season.

On the other hand, based on the data and their behavior, we propose the existence of a permafrost table below the active layer, which top is located at a deep of about 120–140 cm, which mean temperature is near 0 °C, and therefore made it sensible to any environmental change, such as increase of the air temperatures, snow cover changes, and groundwater existence. A possible transitional zone from 100 cm in depth could exist, in agreement with the observations in the thermal data, during the borehole drilling and the mechanical probing to measure the active layer thickness on each thawing season.

SED
6, 679–729, 2014

No trends could be derived from the available thermal data, although a slightly warming of the air and ground appear on the data evolution fitting. Once the thermal characterization has been established by this work, to continue monitoring this CALM site will contribute on the definition of the thermal trend and its evolution, and a deeper borehole will help to confirm the presence of permafrost and to characterize and monitor it.

Acknowledgements. This research was funded by CTM2011-15565-E, CTM2009-10165, and CTM2008-02042-E/ANT projects. Author thank to the Spanish Polar Program, the Spanish Polar Committee, the Unit of Marine Technology and the Spanish Army for their contributions to made possible the develop of the fieldwork campaigns in Byers Peninsula, Antarctica. Our special thanks to mountain guides Hilo and Arkaitz for their support during the fieldwork campaigns. We also thank to Werner Pamler his efforts in the CALM-DAT software development.

References

Andersland, O. B. and Ladanyi, B.: Frozen Ground Engineering, 2nd edn., John Wiley & Sons Inc, UK, 2003.

Bañón, M.: Meteorological observationsat the Spanish Antarctic Base Juan Carlos I., Spanish Ministry of Environment, National Institute of Meteorology, Madrid, 2001 (in Spanish).

Bañón, M., Justel, A., Velázquez, D., and Quesada, A.: Regional weather survey in Byers Peninsula, Livingston Island, South Shetland islands, Antarctica, Antarct. Sci., 25, 146–156, doi:10.1017/S0954102012001046, 2013.

Bjork, S., Hiort, C., Ingolfsson, O., Zale, R., and Ising, J.: Holocene deglaciation chronology from lake sediments, in: Geomorphological Map of Byers Peninsula, Livingston Island, edited by: López-Martínez, J., Thompson, M. R. A., and Thomson, J. W., BAS Geomap Series, Sheet 5-A, Scale 1 : 25 000, British Antarctic Survey, Cambridge, 49–51, 1996.

Bockheim, J. G.: Permafrost distribution in the southern circumpolar region and its relation to the environment: a review and recommendations for further research, Permafrost Periglac., 6, 27–45, 2006.

Bockheim, J. G. and Hinkel, K. M.: Characteristics and significance of the transition zone in drained thaw-lake basins of the Arctic Coastal Plain, Alaska, Arctic, 58, 406–417, 2005.

SED
6, 679–729, 2014

Brown, J., Nelson, F. E., and Hinkel, K. M.: The circumpolar active layer monitoring (CALM) program research designs and initial results, Polar Geography, 3, 165–258, 2000.

Campbell, G. S. and Norman, J. M.: An Introduction to Environmental Biophysics, 2nd edn., Springer, New York, 286 pp., 2000.

de Pablo, M. A., Ramos, M., Vieira, G., and Quesada, A.: A new CALM-S site on Byers Peninsula, Livingston Island, Antarctica, in: Ambientes Periglaciares, Permafrost y Variabilidad Climática: II Congreso Ibérico de la International Permafrost Association, edited by: Blanco, J. J., de Pablo, M. A., and Ramos, M., Servicio de Publicaciones de la Universidad de Alcalá, Alcalá de Henares, 153–159, 2010.

de Pablo, M. A., Blanco, J. J., Molina, A., Ramos, M., Quesada, A., and Vieira, G.: Interannual active layer variability at the Limnopolar Lake CALM site on Byers Peninsula, Livingston Island, Antarctica, Antarct. Sci., 25, 167–180, 2013a.

de Pablo, M. A., Pamler, W., and Ramos, M.: CALM-DAT: software for the analysis of active layer and permafrost thickness, evolution and thermal behavior, First approach, Extended abtracts of the IV Congreso Ibérico de la International Permafrost Association, Vall de Nuria, Spain, in press, 2013b.

Karunaratne, K. C. and Burn, C. R.: Freezing *n*-factors in discontinuous permafrost terrain, Takhini River, Yukon Territory, Canada, in: Proceedings of the 8th International Conference on Permafrost, University of Zurich-Irchel, Zurich, 519–524, 2003.

Karunaratne, K. C. and Burn, C. R.: Relations between air and surface temperature in discontinuous permafrost terrain near Mayo, Yukon Territory, Can. J. Earth Sci., 41, 1437–1451, 2004.

López-Martinez, J., Thomson, M. R. A., and Thomson, S. N. (Eds.): Geomorphological map of Byers Peninsula, Livingston Island, BASGEOMAP Series, Sheet 5-A, Scale 1 : 25 000, British Antarctic Survey, Cambridge, 1996.

Lopez-Martínez, J., Serrano, E., Schmid, T., Mink, S., and Lines, C.: Periglacial processes and landforms in the South Shetland Islands (northern Antarctic Peninsula region), Geomorphology, 155, 62–79, 2012.

Matsuoka, N.: Monitoring periglacial processes: towards construction of a global network, Geomorphology, 80, 20–31, 2006.

Matsuoka, N. and Humlum, O.: Monitoring periglacial processes: new methodology and technology, Permafrost Periglac., 14, 299–303, 2003.

SED
6, 679–729, 2014

Molina, A., de Pablo, M. A., Bardají, T., and Ramos, M.: Caracterización granulométrica y mineralógica de los diferentes tipos de suelos presentes en las islas Livingston y Decepción (Shetland del Sur, Antártida), Extended abtracts of the IV Congreso Ibérico de la International Permafrost Association, Vall de Nuria, Spain, in press, 2013.

Nelson, F. E., Shiklomanov, N. I., Hinkel, K., and Christiansen, H.: Introduction: the Circumpolar Active Layer Monitoring Network (CALM) workshop and CALM II program, Polar Geography, 28, 253–266, 2004.

Otero, X. L., Fernández, S., de Pablo, M. A., Nizoli, E. C., and Quesada, A.: Plant communities as a key factor in biogeochemical processes involving micronutrients (Fe, Mn, Co, and Cu) in Antarctic soils (Byers Peninsula, maritime Antarctica), Geoderma, 195–196, 145–154, 2013.

Pallàs, R., Smellie, J. L., Casas, J. M., and Calvet, J.: Using tephrochronology to date temperate ice: correlation between ice tephras on Livingston Island and eruptive units on Deception Island volcano (South Shetland Islands, Antarctica), Holocene, 11, 149–160, 2001.

Ramos, M. and Vieira, G.: Evaluation of the ground surface Enthalpy balance from bedrock temperatures (Livingston Island, Maritime Antarctic), The Cryosphere, 3, 133–145, doi:10.5194/tc-3-133-2009, 2009.

Ramos, M., Vieira, G., Gilichinsky, D., and de Pablo, M. A.: Establecimiento de estaciones de medida del régimen térmico del permafrost en el área de “Crater Lake”, Isla Decepción (Antártida), in: Ambientes Periglaciares, Permafrost y Variabilidad Climática: II Congreso Ibérico de la International Permafrost Association, edited by: Blanco, J. J., de Pablo, M. A., and Ramos, M., Servicio de Publicaciones de la Universidad de Alcalá, Alcalá de Henares, 93–108, 2009a.

Ramos, M., Hasler, A., Vieira, G., Gruber, S., and Hauck, C.: Setting up boreholes for permafrost thermal monitoring on Livingston Island in the Maritime Antarctic, Permafrost Periglac., 20, 57–64, 2009b.

Ramos, M., de Pablo, M. A., Sebastian, E., Armiens, C., and Gómez-Elvira, J.: Temperature gradient distribution in permafrost active layer, using a prototype of the Ground Temperature Sensor (REMS-MSL) on Deception Island (Antarctica), Cold Reg. Sci. Technol., 72 23–32, 2012.

Ramos, M., de Pablo, M. A., Vieira, G., Molina, A., and Abramov, A.: Interannual active layer thermal and dynamics evolution at the Crater Laker CALM site, Deception Island, Antarctica (2006–2012), Solid Earth, submitted, 2014.

SED
6, 679–729, 2014

Serrano, E., Martínez de Pisón, N. E., and López-Martínez, J.: Periglacial and nival landforms and deposits, in: Geomorphological Map of Byers Peninsula, Livingston Island, edited by: López-Martínez, J., Thompson, M. R. A., and Thomson, J. W., BAS Geomap Series, Sheet 5-A, Scale 1 : 25 000, British Antarctic Survey, Cambridge, 28–34, 1996.

Toro, M., Camacho, A., Rochera, C., Rico, E., Bañón, M., Fernández-Valiente, E., Marco, E., Justel, A., Vincent, W. F., Avendaño, M. C., Ariosa, Y., and Quesada, A.: Limnological characteristics of the freshwater ecosystes of Byers Peninsula, Livingston Island, Antarctica, Polar Biol., 30, 635–649, 2007.

Toro, M., Granados, I., Pla, S., Giralt, S., Antonioades, D., Galán, L., Martínez-Cortizas, A., Lim, H. S., and Appleby, P. G.: Chronostratigraphy of the sedimentary record of Limnopolar Lake, Byers Peninsula, Livingston Island, Antarctica, Antarct. Sci., 26, 198–212, doi:10.1017/S0954102012000788, 2013.

Vieira, G., Bcokheim, J., Gugliemin, M., Balk, M., Abramov, A., Boelhouwers, J., Cannone, N., Ganzert, L., Gilichinsky, D. A., Gotyachkin, S., López-Martínez, J., Meiklejhon, I., Raffi, R., Ramos, M., Schaefer, C., Serrano, E., Simas, F., Sletten, R., and Wagner, D.: Thermal state of permafrost and active-layer monitoring in the Antarctic: advances during the International Polar Year 2007–2009, Permafrost Periglac., 21, 182–197, 2010.

Vila, J., Marti, J., Ortiz, R., Garcia, A., and Correig, A. M.: Volcanic tremors at Deception Island (South Shetland Islands, Antarctica), J. Volcanol. Geotherm. Res., 53, 89–102, 1992.

SED
6, 679–729, 2014

Table 1. Location and characteristics of the sensors installed in the limnopolar Lake CALM site here used for the thermal characterization of the active layer.

Instrument	Sensor	Measurement height/depth (cm)	Frequency (h)	Resolution (˚C)	Accuracy (˚)
Air temperature	Tynitag (Plus 2)	160	1	0.02	0.35
Shallow borehole #1	iButton (DS1922L)	(–) 2.5, 5, 10, 20, 40, 70, 100, 130	3	0.0625	0.50

SED
6, 679–729, 2014

Table 2. Maximum, mean and minimum annual temperatures (in °C) of the air and the ground at different depths (in cm), and calculated range and amplitude.

Measurement	Height/ Depth	Max	Mean	Min	Range	Amplitude
			2009			
Air	160		−3.12			
Ground	−2.5	12.15	−1.3	−5.47	17.62	8.81
	−5	10.21	−1.47	−5.88	16.09	8.045
	−10	8.11	−1.19	−5.43	13.54	6.77
	−20	5.14	−1.19	−4.91	10.05	5.025
	−40	3.13	−1.38	−4.43	7.56	3.78
	−70	1.55	−1.27	−3.5	5.05	2.525
	−100	1.13	−0.93	−2.88	4.01	2.005
	−130	0.61	−0.94	−2.4	3.01	1.505
			2010			
Air	160		−1.74			
Ground	−2.5	14.05	−0.22	−5.37	19.42	9.71
	−5	11.43	−0.23	−4.97	16.4	8.2
	−10	8.34	−0.11	−4.02	12.36	6.18
	−20	6.43	−0.11	−3.08	9.51	4.755
	−40	2.25	−0.19	−1.91	4.16	2.08
	−70	0.91	−0.2	−1.35	2.26	1.13
	−100	0.24	−0.28	−1.27	1.51	0.755
	−130	0.2	−0.22	−1.13	1.33	0.665
			2011			
Air	160		−2.88			
Ground	−2.5	15.42	−1.14	−6.35	21.77	10.885
	−5	12.18	−1.14	−6.18	18.36	9.18
	−10	9.32	−1.09	−5.97	15.29	7.645
	−20	6.08	−1.1	−5.63	11.71	5.855
	−40	2.63	−1.15	−4.85	7.48	3.74
	−70	1.56	−1.1	−3.93	5.49	2.745
	−100	0.62	−1.1	−3.4	4.02	2.01
	−130	0.18	−0.89	−2.71	2.89	1.445
			2012			
Air	160		−2.42			
Ground	−2.5	18.42	−0.58	−8.57	26.99	13.495
	−5	14.45	−0.43	−7.32	21.77	10.885
	−10	12.02	−0.47	−5.71	17.73	8.865
	−20	10.83	−0.4	−3.63	14.46	7.23
	−40	No data	No data	No data	–	–
	−70	2.18	−0.4	−1.66	3.84	1.92
	−100	0.8	−0.35	−1.34	2.14	1.07
	−130	0.31	−0.35	−1.08	1.39	0.695

SED
6, 679–729, 2014

Table 3. Surface and thermal offsets (in ˚C) for each year of the study period.

Measurement	2009	2010	2011	2012
Thermal offset	−0.36	0.00	−0.25	−0.23
Surface offset	−1.82	−1.52	−1.74	−1.84

SED
6, 679–729, 2014

Table 4. Starting date (day/month/year) of the freezing (F) and thawing (T) seasons at different depths (in cm).

Depth	2009	2010		2011		2012	
	F	T	F	T	F	T	F
−2.5	29 Mar 2009	24 Dec 2009	13 Mar 2010	31 Dec 2010	22 Mar 2011	13 Dec 2011	18 Mar 2012
−5	29 Mar 2009	15 Jan 2010	13 Mar 2010	1 Jan 2011	22 Mar 2011	16 Dec 2011	19 Mar 2012
−10	2 Apr 2009	10 Jan 2010	18 Apr 2010	2 Jan 2011	24 Mar 2011	16 Dec 2011	24 Mar 2012
−20	1 Apr 2009	No data	14 Mar 2010	4 Jan 2011	25 Mar 2011	16 Dec 2011	24 Mar 2012
−40	1 Apr 2009	2 Jan 2010	21 Mar 2010	14 Jan 2011	1 Apr 2011	30 Dec 2011	24 Mar 2012
−70	3 Apr 2009	15 Feb 2010	23 Mar 2010	5 Feb 2011	1 Apr 2011	13 Jan 2012	30 Mar 2012
−100	5 Apr 2009	1 Mar 2010	20 Mar 2010	22 Feb 2011	2 Apr 2011	21 Jan 2012	2 Apr 2012
−130	26 Mar 2009	2 Jan 2010	No data	6 Feb 2011	2 Apr 2011	21 Jan 2012	4 Apr 2012

SED
6, 679–729, 2014

Table 5. Length in days of the freezing (F) and thawing (T) seasons at different depths (in cm), and mean value for the studied period.

Depth	2009		2010		2011		2012		Mean	
	T[a]	F	T	F	T	F	T	F[a]	T	F
−2.5	48	270	79	293	81	266	96	310	85.3	284.8
−5	48	292	57	294	80	269	94	309	77.0	291.0
−10	52	283	98	259	81	267	99	304	92.7	278.3
−20	51	296	51	296	80	266	99	304	76.7	290.5
−40	51	276	78	299	77	273	85	No data	80.0	282.7
−70	53	318	36	319	55	287	77	298	56.0	305.5
−100	55	330	19	339	39	294	72	295	43.3	314.5
−130	45	282	79	321	55	294	74	293	69.3	297.5

[a] Season incomplete with the available data.

SED
6, 679–729, 2014

Table 6. Dates (day/month/year) of starting and finishing of the main zero curtain period during the early finish freezing thermal season, and their length in days ([a] period still not finished at 22 January 2013).

Depth	Start	Finish	Length	Start	Finish	Length
			2009			
−2.5	–	–	0	19 Nov 2009	24 Dec 2009	35
−5	–	–	0	19 Nov 2009	15 Jan 2010	57
−10	–	–	0	19 Nov 2009	10 Jan 2010	52
−20	1 Apr 2009	26 Apr 2009	25	20 Nov 2009	22 Jan 2010	63
−40	1 Apr 2009	29 Apr 2009	28	20 Nov 2009	2 Jan 2010	43
−70	3 Apr 2009	13 May 2009	40	20 Nov 2009	15 Feb 2010	87
−100	5 Apr 2009	6 Jun 2009	62	25 Nov 2009	1 Mar 2010	96
−130	26 Mar 2009	15 Jun 2009	81	28 Nov 2009	2 Jan 2010	35
			2010			
−2.5	–	–	0	9 Oct 2010	31 Dec 2010	83
−5	–	–	0	9 Oct 2010	1 Jan 2011	84
−10	–	–	0	9 Oct 2010	2 Jan 2011	85
−20	14 Mar 2010	20 Apr 2010	37	9 Oct 2010	4 Jan 2011	87
−40	21 Mar 2010	2 May 2010	42	9 Oct 2010	14 Jan 2011	97
−70	23 Mar 2010	30 Jun 2010	99	9 Oct 2010	5 Feb 2011	119
−100	20 Mar 2010	9 Jul 2010	111	10 Oct 2010	22 Feb 2011	135
−130	22 Mar 2010	15 Jul 2010	115	3 Dec 2010	6 Feb 2011	65
			2011			
−2.5	–	–	0	7 Oct 2011	13 Dec 2011	67
−5	–	–	0	7 Oct 2011	16 Dec 2011	70
−10	–	–	0	7 Oct 2011	16 Dec 2011	70
−20	25 Mar 2011	4 Apr 2011	10	7 Oct 2011	16 Dec 2011	70
−40	1 Apr 2011	13 Apr 2011	12	8 Oct 2011	30 Dec 2011	83
−70	1 Apr 2011	11 May 2011	40	8 Oct 2011	13 Jan 2012	97
−100	2 Apr 2011	25 May 2011	53	9 Oct 2011	21 Jan 2012	104
−130	2 Apr 2011	10 Jun 2011	69	12 Dec 2011	21 Jan 2012	40
			2012			
−2.5	–	–	0	12 Nov 2012	–[a]	–
−5	19 Mar 2012	23 Mar 2012	4	12 Nov 2012	–	–
−10	24 Mar 2012	1 Apr 2012	8	12 Nov 2012	–	–
−20	24 Mar 2012	4 Apr 2012	11	13 Nov 2012	–	–
−40	24 Mar 2012	No data	–	No data	No data	–
−70	30 Mar 2012	8 Jun 2012	70	14 Nov 2012	–	–
−100	2 Apr 2012	20 Jun 2012	79	15 Nov 2012	–	–
−130	4 Apr 2012	29 Jun 2012	86	12 Nov 2012	–	–

SED
6, 679–729, 2014

Table 7. Thawing and freezing indexes (0 °C day) of air and the ground at different depths (in cm), and resulting difference for each depth and year in the 2009–2012 period.

Experiment	Depth/ Height	2009	2010	2011	2012
		Thawing Index (TDD)			
Air	160	72	91	142	126
Ground	−2.5	143	109	290	264
	−5	133	98	257	252
	−10	148	108	238	241
	−20	139	101	187	222
	−40	103	71	103	No data
	−70	73	47	53	90
	−100	63	16	17	52
	−130	30	23	21	31
		Freezing index (FDD)			
Air	160	−1107	−725	−1167	−1012
Ground	−2.5	−598	−298	−664	−395
	−5	−636	−278	−635	−344
	−10	−558	−235	−612	−342
	−20	−547	−201	−579	−312
	−40	−569	−164	−519	No data
	−70	−503	−128	−442	−223
	−100	−378	−121	−403	−174
	−130	−347	−105	−333	−152
		Difference (FDD – TDD)			
Air	160	−1035	−634	−1025	−886
Ground	−2.5	−455	−189	−374	−131
	−5	−503	−180	−378	−92
	−10	−410	−127	−374	−101
	−20	−408	−100	−392	−90
	−40	−466	−93	−416	
	−70	−430	−81	−389	−133
	−100	−315	−105	−386	−122
	−130	−317	−82	−312	−121

SED
6, 679–729, 2014

Table 8. Slope of TDD and FDD (°C day yr^{-1}) for the air and ground at different depths in the 2009–2012 period.

Slope (°C day yr^{-1})			
Experiment	Depth/ Height	TDD	FDD
Air	160	21.3	15.7
Ground	−2.5	54.4	24.3
	−5	51.6	27.1
	−10	40.9	27.1
	−20	33.5	32.7
	−40	0.0	25.0
	−70	5.7	52.6
	−100	−3.2	33.0
	−130	0.1	35.7
	Mean	23.7	35.7

SED
6, 679–729, 2014

Table 9. Freezing and Thawing indexes (0 °C day) of air and surface, and resulting freezing and thawing *n*-factors (dimensionless) for the different years of the study period, based on calculated mean daily temperatures.

		2009	2010	2011	2012
Air	Thawing Index	72.29	90.86	141.74	126.20
	Freezing Index	−1106.69	−725.35	−1166.94	−1012.44
Surface	Thawing Index	142.67	109.43	290.11	260.27
	Freezing Index	−597.74	−298.21	−663.88	−394.54
n-factor	Freezing	0.54	0.41	0.57	0.39
	Thawing	1.97	1.20	2.05	2.06

SED
6, 679–729, 2014

Table 10. Thermal diffusivity calculated by exponential fitting of thermal amplitude in a selected period of time in which ground temperatures at 2.5, 5, 10 and 20 cm deep show a well defined sinusoidal pattern.

Thermal season	Dates	Thermal diffusivity	R^2
Thawing 2009	25–28 Feb 2009	$4.51 \times 10^{-7} \pm 1.57 \times 10^{-8}\ m^2\ s^{-1}$	0.997
Freezing 2009	–	–	–
Thawing 2010	11–14 Feb 2010	$3.69 \times 10^{-7} \pm 1.74 \times 10^{-8}\ m^2\ s^{-1}$	1.000
Freezing 2010	19–22 Apr 2010	$1.86 \times 10^{-7} \pm 7.83 \times 10^{-8}\ m^2\ s^{-1}$	0.995
Thawing 2011	18–21 Jan 2011	$3.30 \times 10^{-7} \pm 6.81 \times 10^{-8}\ m^2\ s^{-1}$	0.999
Freezing 2011	–	–	–
Thawing 2012	26–30 Dec 2011	$5.56 \times 10^{-7} \pm 9.07 \times 10^{-9}\ m^2\ s^{-1}$	1.000
Freezing 2012	–	–	–

SED
6, 679–729, 2014

Table A1. Limnopolar Lake CALM site definition.

CALM Site	Limnopolar Lake
Site code	A25
Site name	Limnopolar lake
Responsible for data submission	M. A. de Pablo
Email Address	miguelangel.depablo@uah.es
Institution/Organization	Universidad de Alcalá (UAH)
Location description	Limnopolar Lake basin, Byers Peninsula, Livingston Island, Antarctica
Location Lat.	62°38′59.1″ S
Location Lon.	61°06′16.9″ W
Elevation avg. (m)	80
Methods Grid	100 × 100 m
Methods Other	

- air temperature (at 1.6 m high over the surface)
- surface temperature
- ground temperature (2 boreholes: 1.35 and 0.85 cm)
- snow cover (1 mast with array an array of temperature sensors)
- time lapse camera (1 picture per day at noon).
- distributed surface temperature (36 surface temperature sensors distributed in the CALM grid)
- distributed snow cover (9 small masts distributed in the CALM grid with arrays of temperature sensors)
- soils creeping (immediately outside the grid to ensure the non disturbance of the surface during the ALT measurement).

Landscape Description	Outer coastal plain, drained lake basins
Vegetation/Classification	Mostly uncovered. Locally, small mosses patches
Soils (or Material)	Periglacial deposit. Talus scree. Sand to gravel

Thaw depth measurements (year started)	2009
Air temp. measurements (year started)	2009
Snow cover measurements (year started)	2009
Distributed snow cover measurements (year started)	2013
Surface temp. measurements (year started)	2009
Distributed surface temp. measurements (year started)	2012
Ground temp. measurements (year started)	2009
Time lapse camera (year started)	2009
Soil creeping (year started)	2012

SED
6, 679–729, 2014

Table A1. Continued.

General description of soil moisture (dry, moist, wet, saturated)	Dry to wet, depending of the sector of the CALM site. Saturated at selected nodes.
Soil texture: if non organic describe texture, if organic indicate thickness of organic layer (cm)	Not organic layer; Mineral texture – variable from sandy load to coarse gravel. Some nodes are silts
Additional information	
Additional thaw depth measurements are done in (A) 3 sites 1 × 1 m grid (9 nodes) at different locations inside the CALM site grid, measured every two days to see the evolution of soil thaw; (B) 1 detail site 10 × 10 m (36 nodes) of a representative sector of the main CALM site, to provide a more detailed measurements of the Active Layer evolution. Those additional measurements are carried out when there is enough available time during the Antarctic campaign in the protected region of Byers Peninsula. During the ALT measurement by mechanical probing of the Limnopolar Lake CALM site, additional measurements of surface and soil temperatures, and surface and subsurface (5 cm depth) unconfined unconsolidated not drained soils resistance, are also done in each node, when available time during the Antarctic campaign.	
Soil description:	
Sand to gravel	
Sampling design and method:	
100 × 100 m grid surveyed and permanently staked in the edge by stakes separated by 10 m, yielding an 11 × 11 array of sampling nodes. Thaw depth sampling was conducted twice by manual probing at each node of the grid. The two values for each sampling point are averaged, yielding a maximum of 121 data points per grid per probing date during the thaw season (normally last days of Jan or early Feb, due to logistical requirements during Antarctic campaigns). The active layer was not measured at locations where grid points are covered by thick layer of ice and snow, since the ground remains frozen.	
Other information	
We have instrument measuring different parameters: air temperature (hourly measurements by tinytag device by Gemini), surface temperature (3 h measurements byiButton devices from Maxim), snow thickness (based on the use of an array of temperature sensors mounted on a wood mast at 2.5, 5, 10, 20, 40, 80, and 160 cm high byiButton devices), and ground temperature, at 2 boreholes of 135 cm and 85 cm depth. Measurements are done at 2.5, 5, 10, 20, 40 70, 100, and 130 cm, and 2.5, 5, 10, 20, 40, 70, and 80 cm, respectively, by iButton devices. Moreover, we installed 9 small masts regularly distributed in the CALM site to derive snow thickness. 36 temperatures sensors, regularly distributed in the CALM site also measure surface temperature along the grid. A meteorological station was installed in 2006 by other research team who search their data with us to complete our data. A time lapse camera acquire one image per day of the CALM site and surrounding area in order to observe the evolution of weather, snow coverage and watersheet of the near Limnopolar lake.	

SED
6, 679–729, 2014

Table A1. Continued.

References

- de Pablo, M. A., Blanco, J. J., Molina, A., Ramos, M., Quesada, A., and Vieira, G.: Interannual active layer variability at the Limnopolar Lake CALM site on Byers Peninsula, Livingston Island, Antarctica, Antarct. Sci., 25, 167–180, doi:10.1017/S0954102012000818, 2013.
- Otero, X. L., Fernández, S., de Pablo, M. A., Nizoli, E. C., and Quesada, A.: Plant communities as a key factor in biogeochemical processes involving micronutrients (Fe, Mn, Co, and Cu) in Antarctic soils (Byers Peninsula, maritime Antarctica), Geoderma, 195–196, 145–154, 2013.
- de Pablo,M. A., Ramos, M., and Molina, A.: Active Layer evolution (2009–2011) at "Limnopolar Lake" CALM-S site on Byers Peninsula, Livingston Island (Antarctica), in: III-Congreso Ibérico de la IPA, Piornedo, Spain, Abstracts, 2011.
- de Pablo, M. A., Ramos, M., Vieira, G., Toro, M., and Quesada, A.: Preliminary results from "Limnopolar" Lake CALM-S site experience, Byers Peninsula, Livingston Island (Antarctica), International Polar Year – Oslo Science Conference, Oslo, Norway, Abstracts, 2010.

Data

Year	2009	2010	2011	2012	2013 2014
Mean Active layer thickness (cm):	46.8	43.4	40.5	39.1	11.7
Mean Air temperature (°C):	−2.91	−1.61	−3.07	−2.46	–
Mean Surface temperature (°C):	−1.40	−0.62	−1.08	−0.11	–
Maximum snow cover (°C):	80	80	40	80	–

SED
6, 679–729, 2014

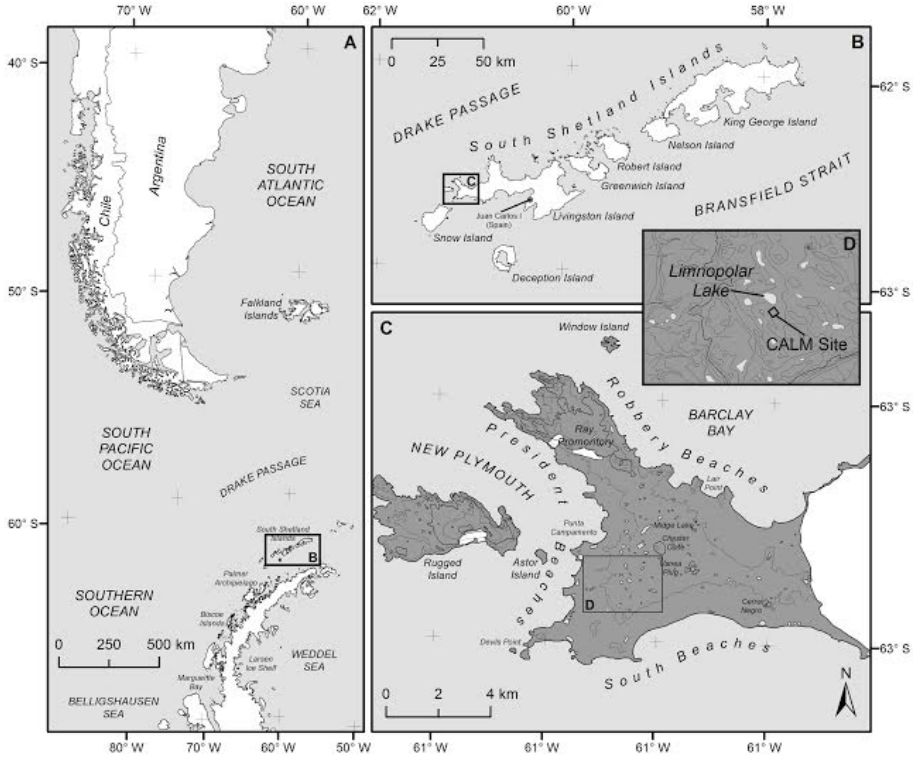

Fig. 1. Location of the Limnopolar Lake CALM site (A25) in Byers Peninsula, Livingston Island, in the South Shetland Archipelago, Antarctica.

SED
6, 679–729, 2014

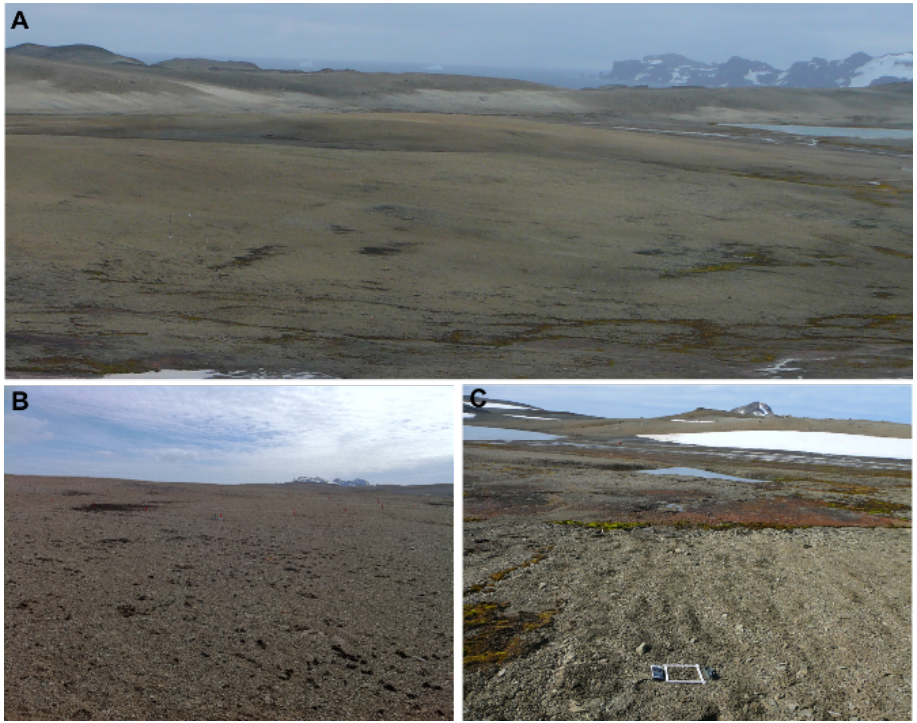

Fig. 2. (A) Picture of the area in which the CALM site is located at the SW flank of the Limnopolar Lake, in a smooth and gently sloped (< 2 %) terrain without vegetal coverage. The surface is characterized by fine to coarse materials **(B)**, sometimes organize din pattern ed grounds, with presence of ponds and small mosses patches **(C)**.

SED
6, 679–729, 2014

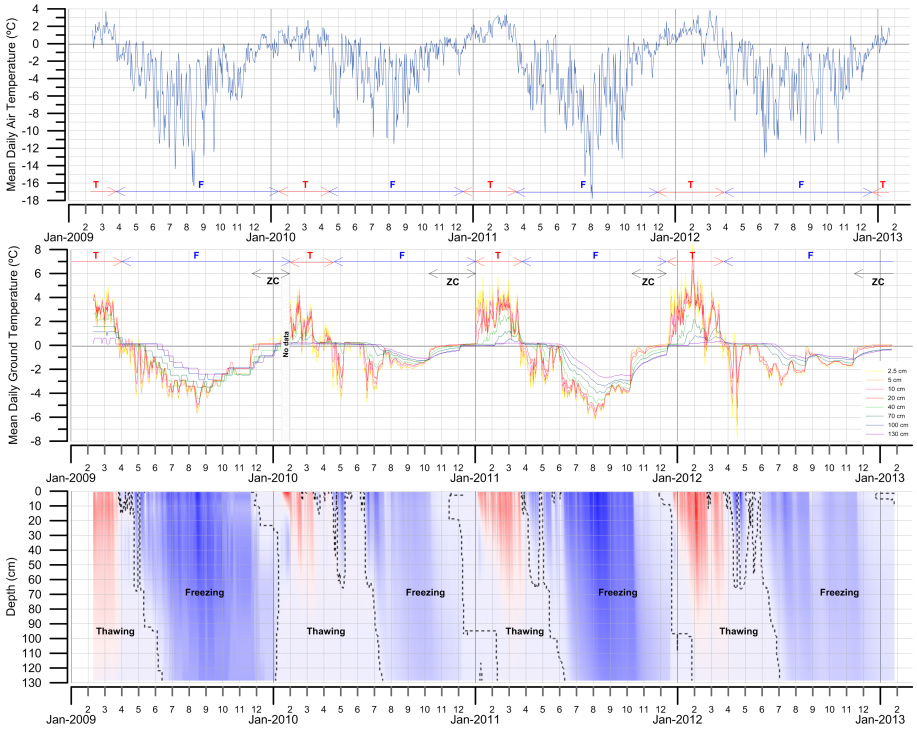

Fig. 3. Mean daily temperature data of the air (top) and the ground at different depths in the 130 cm depth borehole (middle) of the Limnopolar Lake CALM site, and resulting thermogram for the monitoring period (bottom).

SED
6, 679–729, 2014

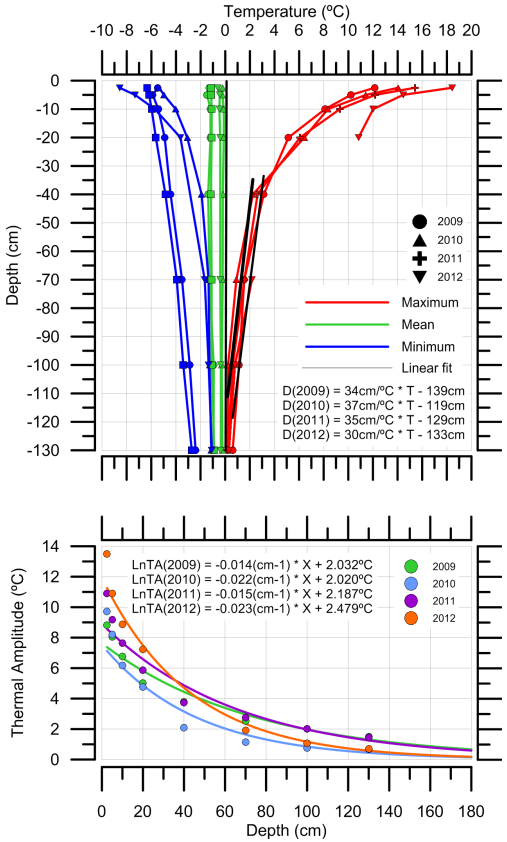

Fig. 4. (Top) Thermal profiles showing minimum (blue), mean (green) and maximum (red) temperatures of the ground at different depths in 2009, 2010, 2011 and 2012, and equations of the linear fitting curve to the maximum temperatures. (Bottom) Exponential fitting curves to the thermal amplitudes of the ground at different depths, and their corresponding equations, to calculate the top of the permafrost depth.

SED
6, 679–729, 2014

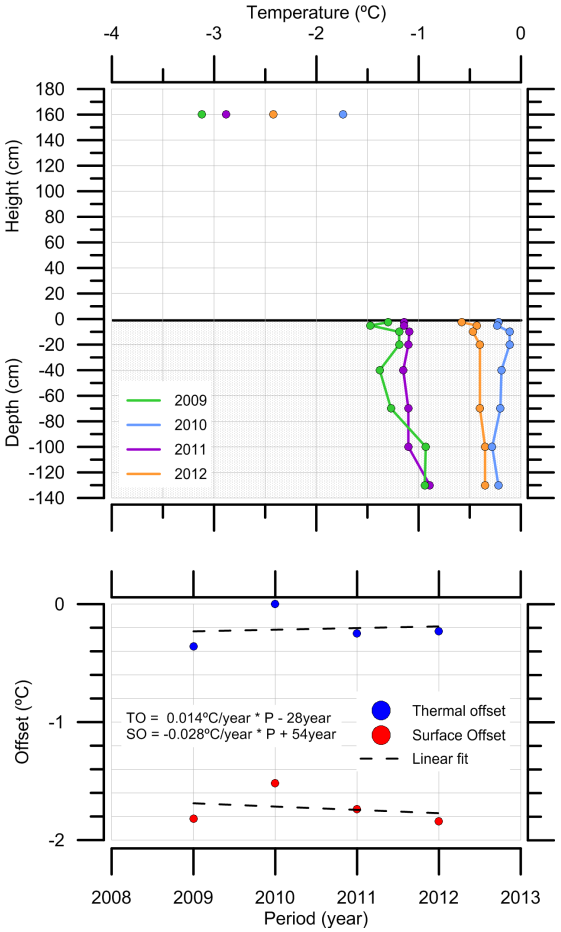

Fig. 5. Mean annual air and ground temperatures at different depths used to derive the thermal and surface offset (top), and their evolution along the study period (bottom).

SED
6, 679–729, 2014

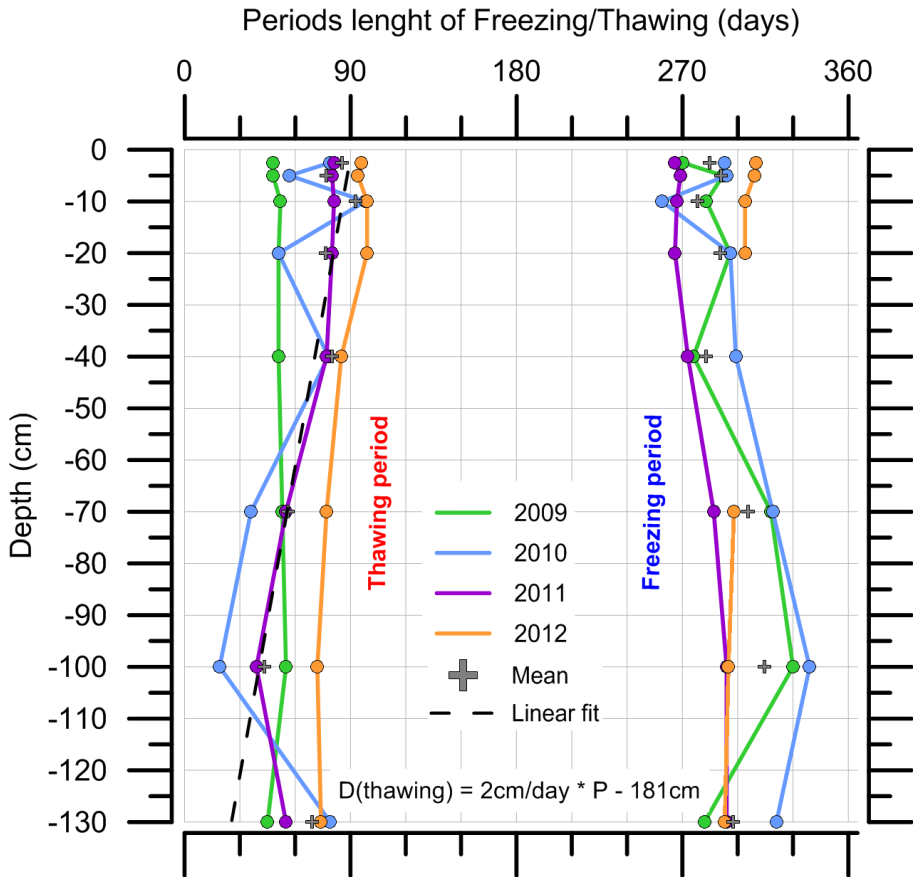

Fig. 6. Freezing and thawing periods lengths (in days) for each year of the study period, and linear fitting used to derive the depth in which grounds does not have thaw processes, i.e., the depth of the top of the permafrost.

SED
6, 679–729, 2014

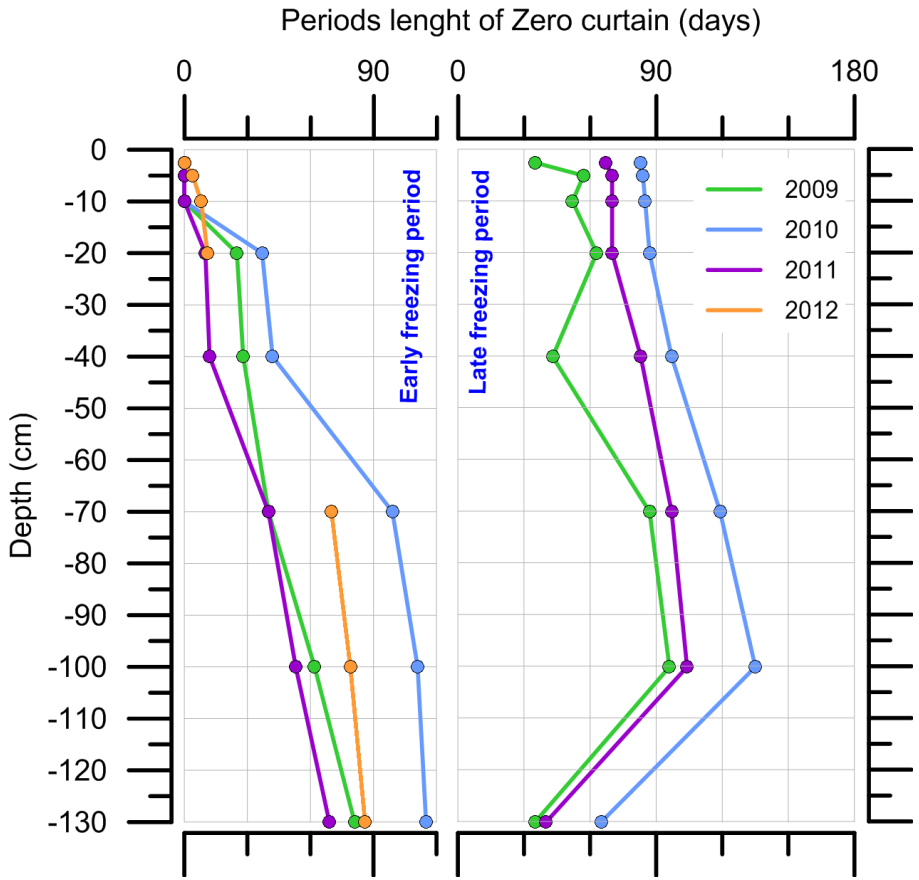

Fig. 7. Length (in days) of the zero curtain periods at different depths during the early (left) and late (right) freezing period.

SED
6, 679–729, 2014

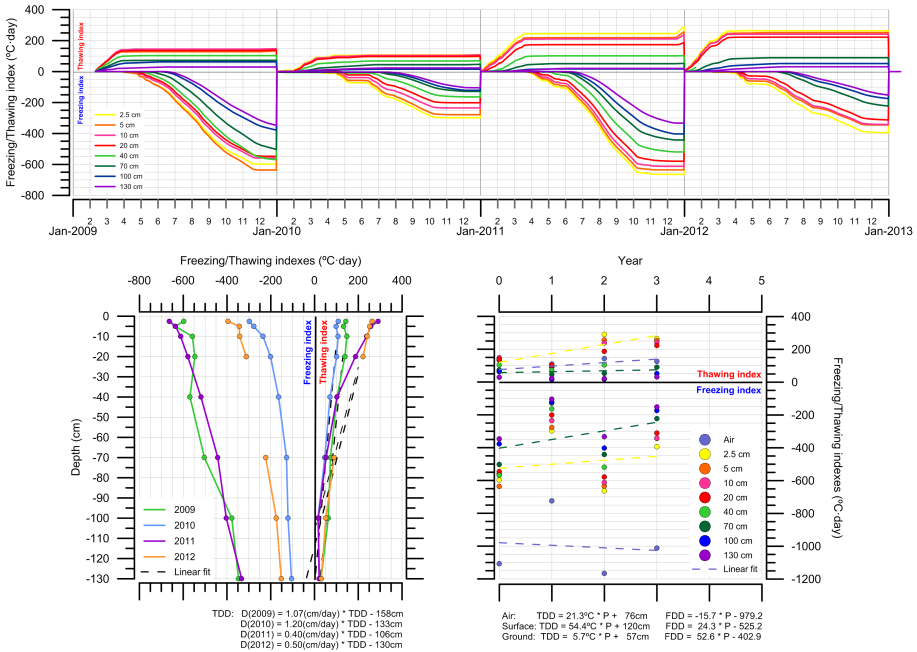

Fig. 8. Annual accumulated FDD and TDD indexes for the ground at different depths (top), and their evolution in the study period (bottom right) with linear fitting curves for the air, surface and 70 cm in depth. FDD and TDD profiles (bottom left) allow to deduce a negative balance for each year, and linear fitting to TDD allow to deduce the theoretical depth with null thawing, i.e., depth of the top of the permafrost.

SED
6, 679–729, 2014

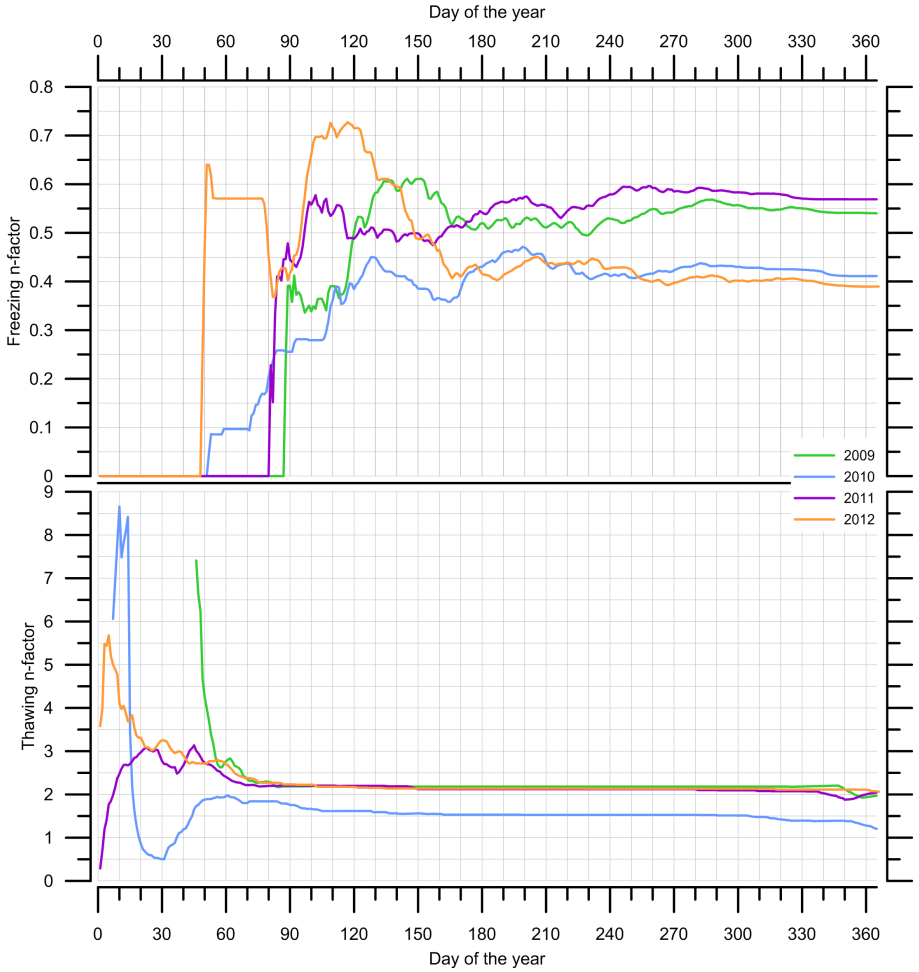

Fig. 9. Freezing (top) and thawing (bottom) *n*-factors for the different years.

SED
6, 679–729, 2014